Effect of suspended solids on peracetic acid decay and bacterial inactivation kinetics: Experimental assessment and definition of predictive models

Laura Domínguez Henao, Matteo Cascio, Andrea Turolla, Manuela Antonelli *

Politecnico di Milano, Department of Civil and Environmental Engineering (DICA) - Environmental Section, Piazza Leonardo da Vinci 32, 20133 Milano, Italy

The work addresses the effect of total suspended solids (TSS) on disinfection by peracetic acid (PAA) concerning both PAA decay and bacterial inactivation kinetics. The effect of TSS on PAA decay was evaluated at five TSS con-centrations (5, 40, 80, 120 and 160 mg/L), obtained from stock TSS solutions prepared from activated sludge sam-ples. The influence of the soluble matter associated to the suspended solids on PAA decay was evaluated separately, using the same stock TSS solution after the removal of solids by filtration. The contributions of suspended and soluble fractions were found to be independent, and a predictive model formed by two additive sub-models was proposed to describe the overall PAA decay kinetics. Moreover, an uncertainty analysis was per-formed by a series of Monte Carlo simulations to propagate the uncertainties associated to the coefficients of the model. Then, the disinfectant dose (mg/L min) was highlighted as the main parameter determining disinfection efficiency on a pure culture of *E. coli* and an inactivation kinetic model was developed based on the response of *E. coli* to various PAA doses. Finally, the effect of TSS (40 and 160 mg/L) on the inactivation of free-swimming *E. coli* was investigated at two PAA doses (5 and 20 mg/L min). TSS reduced inactivation extent an average of 0.4 logs at 5 mg/L min and 1.5 logs at 20 mg/L min. It was hypothesized that this might be due to the formation of bacteria aggregates as defense mechanism against disinfection, enhanced by the presence of solids.

Keywords: Disinfection, Peracetic acid, *Escherichia coli*, Suspended solids, Decay rate kinetics, Bacterial inactivation kinetics, Exposure dose

G R A P H I C A L A B S T R A C T

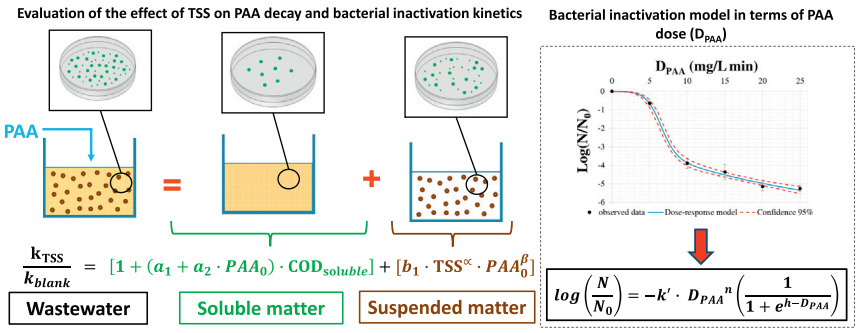

H I G H L I G H T S

- TSS concentrations higher than usual values of secondary effluents affect PAA decay.
- The effect of soluble matter associated to TSS is less relevant for PAA decay.
- Exposure dose is a reliable parameter to describe PAA disinfection performance.
- The presence of TSS decreases PAA dis-infection efficiency.

1. Introduction

Disinfection is a key process in wastewater treatment and it plays a fundamental role in public health protection. Peracetic acid (PAA) gained momentum over the last decades as disinfectant for wastewater

Article history:
Received 12 April 2018
Received in revised form 25 May 2018
Accepted 18 June 2018
Available online xxxx

Editor: Ching-Hua Huang

* Corresponding author.
E-mail address: manuela.antonelli@polimi.it (M. Antonelli).

Nomenclature

PAA	peracetic acid
CSO	combined sewer overflow
WWTP	wastewater treatment plant
TSS	total suspended solids (mg/L)
PAB	particle associated bacteria
E. coli	*Escherichia coli*
D_{PAA}	peracetic acid dose (mg/L min)
MBBR	moving bed biofilm reactor
CAS	conventional activated sludge
BOD	biological oxygen demand (mg/L)
COD	chemical oxygen demand (mg/L)
Ntot	total nitrogen (mg/L)
PO_4^{3-}	phosphate (mg/L)
CFU	colony forming units
N_0	initial number of bacteria before disinfection (CFU/mL)
N	number of bacteria after disinfection (CFU/mL)
ABS	absorbance
y, z	coefficients of the standard curve for PAA measurement
PAA0	initial PAA concentration (mg/L)
PAAt	PAA concentration at time t (mg/L)
OD	oxidative demand (mg_{PAA}/L)
t	contact time (min)
k	decay rate constant (min^{-1})
k_{blank}	blank decay rate constant (min^{-1})
k_{sol}	decay rate constant ascribable to the soluble matter (min^{-1})
k_{TSS}	decay rate constant ascribable to the suspended and soluble matter (min^{-1})
k^*	decay rate constant ascribable to the suspended matter (min^{-1})
	a_1, a_2, b_1, α, β coefficients of the non-linear regression
k'	bacterial inactivation rate constant
n, m, *x*	parameters of the generalized inactivation rate (GIR) model
C	disinfectant concentration in the GIR model (mg/L)
h	parameter of the *E. coli* inactivation model

due to its powerful antimicrobial activity (Kitis, 2004; Luukkonen et al., 2014) combined with a limited formation of disinfection by-products (Dell'Erba et al., 2007; Liberti and Notarnicola, 1999), even in case of poor quality of the water matrix, as for combined sewer overflows (CSOs) disinfection (US EPA, 1999). However, PAA decays rapidly in aqueous solutions (Yuan et al., 1997). Previous studies suggested that the water matrix composition, particularly organic and suspended matter content, has a significant influence on PAA decay, as readily oxidable compounds immediately consume the disinfectant (Falsanisi et al., 2006; Koivunen and Heinonen-Tanski, 2005; Lazarova et al., 1998; Liu et al., 2014; Pedersen et al., 2013). Therefore, guarantying a sufficient amount of disinfectant to reach bacterial inactivation targets, while avoiding high residuals at effluent discharge, is a key objective in the design and operation of effective disinfection systems.

Suspended solids in wastewater treatment plants (WWTPs) include a wide and heterogeneous group of particles whose characteristics and composition are determined by a combination of factors, including the characteristics of the influent wastewater, which mainly depend on the source (domestic, industrial, agricultural, storm) and on the type of the sewer (combined or separated), and the treatment processes occurring in the WWTP. A key element when dealing with suspended solids is the particle structure, that is not smooth and rigid but rather an irregular sponge-like matrix characterized by pores of different sizes in which bacteria can be shielded (Dietrich et al., 2003).

Suspended solids affect PAA disinfection mainly by two mechanisms: (i) consumption of PAA entailing a reduction of the available concentration for disinfection and, thus, a lower PAA exposure dose for bacteria inactivation, and (ii) shielding of bacteria against the action of the disinfectant.

As for PAA decay, previous works investigated the contribution of soluble organic content in terms of macro-parameters such as chemical oxygen demand (COD) and biological oxygen demand (BOD), while the effect of suspended matter has been scarcely studied, although it has been observed in different works (Chhetri et al., 2016, 2014; Falsanisi et al., 2008; Koivunen and Heinonen-Tanski, 2005; Lazarova et al., 1998; Lefevre et al., 1992; McFadden et al., 2017; Sánchez-Ruiz et al., 1995; Stampi et al., 2001). Several authors have indicated that primary effluents and CSOs require higher PAA concentrations for disinfection than secondary and tertiary effluents (Chhetri et al., 2016; Gehr and Cochrane, 2002; Koivunen and Heinonen-Tanski, 2005; Luukkonen et al., 2014). Furthermore, Chhetri et al. (2016) observed that a pre-treatment of CSO for the removal of suspended solids decreases the required disinfectant dosage.

Regarding the protective shielding afforded to bacteria, suspended solids play a major role. Microbial aggregates and microorganisms attached to or embedded into particles demonstrated increased resistance to inactivation by different disinfectants compared to non-attached, free-swimming microorganisms (Bohrerova and Linden, 2006; Dietrich et al., 2007; LeChevallier et al., 1984; Winward et al., 2008). However, it should be considered that approximately 99% of the overall bacterial population in wastewater is free-swimming (i.e., bacteria size < 10 μm) and only approximately 1% or less consists of particle associated bacteria (PAB) (Falsanisi et al., 2008; Qualls et al., 1985, 1983). As for the particle size of suspended solids, Falsanisi et al. (2008) observed that it has a paramount importance during PAA disinfection, as the protection afforded by TSS was 0.6 and 1.3 logs for solids between 10 and 120 μm and >120 μm, respectively, whereas McFadden et al. (2017) observed that solid size in the range between 10 and 100 μm had a minor effect on PAA disinfection. A decrease in disinfection efficiency of PAA with increasing TSS concentrations has been observed in previous works (Kitis, 2004; McFadden et al., 2017); however, limited research has been conducted to elucidate this aspect. Stampi et al. (2001) reported that the detrimental impact on PAA disinfection performance is moderate and constant for TSS concentrations between 10 and 40 mg/L, while Lefevre et al. (1992) found that PAA presents an excellent disinfection performance even up to 100 mg/L.

When dealing with PAA disinfection, another key aspect is related to the actual dose (mg/L min) as the main parameter determining disinfection efficiency, whose estimation must depend on the changing concentration of disinfectant at which bacteria are exposed over contact time (Santoro et al., 2015). Usually the design and operation of disinfection processes with chlorine-based compounds, for simplicity, is based on the estimation of the exposure dose calculated as the product of initial disinfectant concentration and contact time. Consequently, the most widely used inactivation models are based on this concept and therefore on these two parameters. However, this approach neglects the disinfectant decay, thus it is not a reliable predictor for PAA disinfection performance. On the contrary, PAA decay should be considered in the calculation of the actual PAA dose (D_{PAA}), considering the disinfectant active concentration at any contact time (Haas and Joffe, 1994; Turolla et al., 2017).

The present study aims at elucidating the effect of suspended solids on PAA decay and *E. coli* inactivation performance. PAA decay was assessed in the presence of five different TSS concentrations (5, 40, 80, 120 and 160 mg/L), representing secondary effluents of good (well settled) and medium (not well-settled) quality, and CSOs. In detail, stock TSS solutions were prepared from activated sludge samples to obtain test solutions at different TSS concentrations. In addition, the effect on PAA decay of the soluble matter in solution with suspended solids was also evaluated, after removing the solids by filtration at 0.45 μm. A

Table 1
Physical-chemical characteristics of the stock TSS and filtrate solutions.

Parameter		WWTP-A		WWTP-B	
		Stock TSS solution	Stock filtrate solution	Stock TSS solution	Stock filtrate solution
Particle size (mean ± st.dev.)	μm	1.013 ± 0.127	–	1.568 ± 0.881	–
UV_{254}	cm^{-1}	0.292	0.057	0.168	0.047
TSS	mg/L	450	–	240	–
COD	mg/L	408	195	204	137
N_{tot}	mg_N/L	22	12	17	9.9
PO_4^{3-}	mg_P/L	5.2	3	0.85	0.37

mathematical model to relate TSS concentration and residual concentration of PAA was developed, considering the contribution of suspended and soluble matter. Then, the effect of TSS on PAA disinfection efficiency has also been addressed. For this latter purpose, firstly PAA dose was validated as the main parameter determining disinfection efficiency. The dose-response curve of a pure culture of *E. coli* in saline solution was determined and a log-inactivation model to describe *E. coli* inactivation as a function of the actual disinfectant dose was studied. The independence of the extent of bacterial inactivation from the operating conditions was tested by exposing bacteria to same PAA doses obtained with different combinations of initial PAA concentration and contact time (t). Finally, the effect of TSS on PAA disinfection was assessed at two PAA doses in order to verify the existence of a potential defense mechanism for bacteria against disinfection afforded by TSS. For instance, TSS possibly might act as a condensation nucleus that favors aggregation of bacteria, as proposed in previous works (Bohrerova and Linden, 2006; Mir et al., 1997; Turolla et al., 2017).

2. Materials and methods

2.1. Reagents

PAA technical grade solution (VigorOx® WWTII) was supplied by PeroxyChem, whose composition as weight percentage is 15% of peracetic acid, 23% of hydrogen peroxide and 16% of acetic acid. The PAA concentration in the commercial solution was checked monthly by iodometric titration (Sully and Williams, 1962). The LB broth (10 g/L of tryptone, 5 g/L of yeast extract and 5 g/L of NaCl) and the saline solution (9 g/L of NaCl) were prepared in deionized water and sterilized in autoclave at 120 °C for 20 min. All chemicals were reagent grade purchased from Sigma Aldrich, except for DPD (N,N-diethyl-*p*-phenylenediaminesulfate) salt and test kits that were provided by Hach Lange, whereas tryptone, yeast extract and C-EC Agar were supplied by Biolife.

2.2. Preparation of stock TSS and filtrate solutions

Activated sludge samples were collected from two conventional municipal wastewater treatment plants in Milan area (WWTP-A and -B, respectively). Both WWTPs are based on a treatment train composed of preliminary treatments, denitrification/nitrification biological reactors and clarification tanks. The WWTPs have different configurations of the biological process: WWTP-A is equipped with a conventional activated sludge (CAS) biological reactor with suspended biomass, while WWTP-B combines CAS reactor with a Moving Bed Biofilm Reactor (MBBR) in which biomass additionally grows immobilized on plastic media. The activated sludge samples were collected in the aeration basins.

The concentrated stock TSS solutions were prepared by collecting the supernatant of the activated sludge samples after 2 h of settling, which was assumed to be representative of the suspended solids in a secondary effluent before disinfection. The soluble fraction associated to the stock TSS solution (stock filtrate solution) was obtained by filtering a portion of the stock TSS solution using acetate-cellulose membranes (0.45 μm pore size, Sartorius). Both stock solutions were sterilized at 120 °C for 30 min. The stock TSS solutions were analyzed for particle size distribution, absorbance at 254 nm (UV_{254}), TSS, COD, total nitrogen (N_{Tot}) and phosphate ion (PO_4^{3-}) concentrations, while the stock filtrate solutions were analyzed for UV_{254}, COD, total nitrogen and phosphate ion concentrations, as summarized in Table 1. No significant changes were observed in particle size distribution after sterilization. Stock solutions were stored in the dark and at 4 °C for up to two weeks.

2.3. E. coli pure culture preparation and cell enumeration

The *E. coli* (DH5α) pure culture was provided by the Laboratory of Environmental Engineering of the Politecnico di Milano (LIA) and it was grown to exponential phase overnight in LB broth incubated at 37 °C for 24 h in an orbital incubator SI600 (Stuart) with continuous shaking speed at 90 rpm. *E. coli* cells were centrifuged for 20 min at 4000 rpm, washed and re-suspended three times with saline solution to achieve a cell count of approximately 10^8 to 10^9 CFU/mL. The number of cells in the washed cell suspension was roughly estimated by measuring the optical density at 600 nm (Unicam UV/VIS 2 - optical path 10 mm) and the viable cells were enumerated as colony forming units by single plate-serial dilution spotting (SP-SDS) on chromogenic substrate C-EC Agar (Biolife) after incubation at 37 °C for 18–24 h.

2.4. Experiments on PAA decay

1-h decay tests were performed in completely mixed batch reactors (1 L) mixed by magnetic stirrer (380 rpm) in dark conditions at room temperature (20 ± 1 °C). As for the assessment of the influence of TSS on PAA decay, the stock TSS solution was diluted in deionized water to obtain five different TSS concentrations (5, 40, 80, 120 and 160 mg/L) and the effect on PAA decay was tested at three different initial concentrations of PAA (2, 5 and 8 mg/L). The stock filtrate solutions were prepared adopting the same dilution factors of the stock TSS solution in order to obtain the equivalent concentration of soluble matter associated to each TSS concentration. The pH of the solutions was adjusted to 7.5 at the beginning of the tests with sodium hydroxide (NaOH, 1 M) or sulfuric acid (H_2SO_4, 1 M), and it was monitored continuously (EcoScan pH6, Eutech Instruments). Samples were collected at five contact times (2, 5, 10, 30 and 60 min) to measure the residual PAA concentration. As for the blank decay of PAA at 2 and 5 mg/L, values determined in a previous work (Domínguez Henao et al., 2018) were adopted, whereas the blank decay at 8 mg/L was estimated by means of the equation reported by the cited authors and confirmed by PAA decay tests carried out using the same setup as the aforementioned experiments. All the experiments were repeated in triplicate.

2.5. Experiments on E. coli inactivation

1-hour disinfection tests were performed in Erlenmeyer flasks of 500 mL where an aliquot of 25 μL of the washed cell suspension was inoculated into 250 mL of test solution, to reach an *E. coli* count of 10^6

Table 2
PAA doses (D_{PAA}) and combinations (PAA_0, t) of initial concentration of PAA (mg/L) and contact time (min) tested. The dose-response curve was built using the underlined combinations.

Test solution	Combination #	D_{PAA} (mg/L min)				
		5	10	15	20	25
Saline solution	1	0.50, 10	–	–	2.00, 10	–
	2	0.25, 20	0.50, 20	–	1.01, 20	–
	3	0.17, 30	–	0.50, 30	0.68, 30	–
	4	0.11, 45	–	–	0.50, 41	–
	5	0.09, 60	–	–	0.35, 60	0.50, 52
40 mg_{TSS}/L		0.50, 13	–	–	1.00, 11	–
160 mg_{TSS}/L		1.00, 22	–	–	2.00, 29	–

CFU/100 mL approximately. Table 2 shows the experimental plan for *E. coli* disinfection. In detail, the relation between the applied PAA dose and the resulting *E. coli* inactivation (dose-response curve) was determined in saline solution at five PAA doses (5, 10, 15, 20 and 25 mg/L min). The independence of the extent of bacterial inactivation from the operating conditions was tested at three PAA doses (5, 10 and 20 mg/L min) varying the initial concentration of PAA (PAA_0, in mg/L) and contact time (t, min), according to the combinations shown in Table 2. Regarding the evaluation of the effect of TSS on the disinfection performance of PAA, it was tested at two TSS concentrations (40 and 160 mg/L), solely with the stock TSS solution prepared with the activated sludge from WWTP-A.

The extent of bacterial inactivation after disinfection tests was expressed as the log-inactivation of viable colony forming units, log (N/N_0), where N_0 and N are the microbial densities before and after disinfection, respectively. Each disinfection test was replicated four times.

2.6. Analytical procedures

The size distribution of stock TSS solutions was determined using Zetasizer Nano ZS90 (Malvern). The concentrations of TSS were measured according to Standard Methods (APHA/AWA/WEF, 2012) using 0.45 μm acetate-cellulose membranes (Sartorius). COD, total nitrogen and phosphate ion were measured using test kits (LCK 114, 138, 349 respectively) and a spectrophotometer Dr. Lange XION 500 (Hach Lange).

PAA residual concentrations were measured by the DPD method according to Domínguez-Henao et al. (2018). The absorbance was measured by a Unicam UV/VIS 2 spectrophotometer at 530 nm (optical path 40 mm). The interference of the suspended solids with spectrophotometric measures due to light scattering was corrected by filtering the samples on syringe filters (0.45 μm acetate-cellulose membranes) prior to the absorbance measure.

Samples for microbiological analyses were collected in sterile flasks, after the addition of 0.5 mL sodium thiosulfate (0.1 N) and 0.5 mL of bovine catalase solution (600 units/mL) to quench residual PAA and H_2O_2, respectively. Microbiological analyses were performed in two dilutions, each one repeated twice. *E. coli* were enumerated by plate-count standard technique based on a membrane filtration procedure (method 7030C, APAT-IRSA/CNR, 2003) using sterile mixed cellulose esters membrane (GN-6 Metricel® MCE Membrane Disc Filters, Pall). *E. coli* were cultured on chromogenic substrate C-EC agar and incubated at 37 °C for 18–24 h. The colonies of *E. coli* were evidenced as green-blue colonies, fluorescent under the light of a Wood lamp (365 nm). Results were expressed as colony forming units (CFU) in a reference volume of 100 mL (CFU/100 mL).

2.7. Data processing

The standard curve for PAA measurement was obtained through a linear least-square regression ($R^2 = 0.9995$). The equation was $ABS_{530} = y + z \cdot PAA$, where ABS is the absorbance value at 530 nm and PAA is the concentration of PAA (mg/L). The estimated coefficients are $y = 0.0624$, $z = 0.5563$. The residual PAA concentrations measured during decay tests were plotted over time for each experiment (residual PAA concentrations at five contact times in triplicate, for a total of 15 data) and interpolated with a non-linear least-square regression according to a modified first-order kinetic model proposed by Haas and Finch (2001) (Eq. (1)).

$$PAA_t = (PAA_o - OD) \cdot e^{-kt} \quad (1)$$

where PAA_0 is the initial PAA concentration (mg/L), PAA_t is the concentration at time t, k is the decay rate constant (min^{-1}) and OD is the initial oxidative demand (mg/L).

PAA dose (D_{PAA}) was quantified by estimating the area under the PAA decay curve until a defined contact time (min) as in Eq. (2) (Santoro et al., 2015):

$$D_{PAA} = \int_0^t (PAA_o - OD) \cdot e^{-k \cdot t} dt = \frac{(PAA_0 - OD)}{k} \cdot \left(1 - e^{-k \cdot t}\right) \quad (2)$$

The estimation of regression coefficients and the Monte Carlo simulations were performed in Mathworks Matlab R2017a, while the statistical analysis was performed using Minitab 17.

3. Results and discussion

3.1. Effect of TSS on PAA decay

Experimental tests on TSS solutions accounted for the contribution of suspended and soluble matter, whereas experiments with filtrate solutions permitted to consider only the contribution of soluble matter. Raw data from experimental tests and related fitting by the Haas and Finch kinetic model are shown in Fig. S1 of Supporting Material, while the values of initial oxidative demand (OD) and decay rate constant (k) estimated by the non-linear least-square regression are reported in Supporting Material (Tables S1 and S2 for WWTP-A and B, respectively). In the following sections, estimated values are discussed.

3.1.1. Initial oxidative demand

The soluble matter associated to TSS exhibited scarce initial oxidative demand, ranging from −0.8% to 4.9% and from −0.5% to 7.9% of initial PAA concentration for solutions prepared with the activated sludge from WWTP-A and WWTP-B, respectively. In contrast, the estimated values for initial oxidative demand due to TSS can be grouped in two clusters. The first one corresponds to the experiments on TSS concentrations between 5 and 40 mg/L, for which the initial oxidative demand is not affected by the presence of solids. These values are similar to those observed in the experiments performed on the associated soluble fractions. The second cluster corresponds to the experiments on TSS concentrations of 80, 120 and 160 mg/L, for which the presence of TSS led to significantly higher initial oxidative demand with respect to the associated soluble fraction. Furthermore, for TSS concentrations higher than 80 mg/L the initial oxidative demand was independent of TSS concentration, while it depended on the initial PAA concentration. In detail, initial oxidative demand values of 0.4 and 0.8 mg/L were observed for 2 and 5 mg/L and for 8 mg/L, respectively. This finding suggests that the limiting factor in the rapid oxidation reactions occurring between PAA and organic matter is represented by PAA concentration.

3.1.2. Decay rate constant

Regarding the effect of TSS and associated soluble fraction on the decay rate constant, an increasing trend with TSS concentrations was observed. Fig. 1 summarizes the estimated values, referred to as k_{TSS} and k_{sol} for the experiments performed on TSS and filtrate solutions, respectively. The effect of low concentrations of both suspended and soluble matter on PAA decay was negligible and comparable to the blank decay of PAA (shown in Fig. S1 in Supporting material). In detail, k_{TSS}

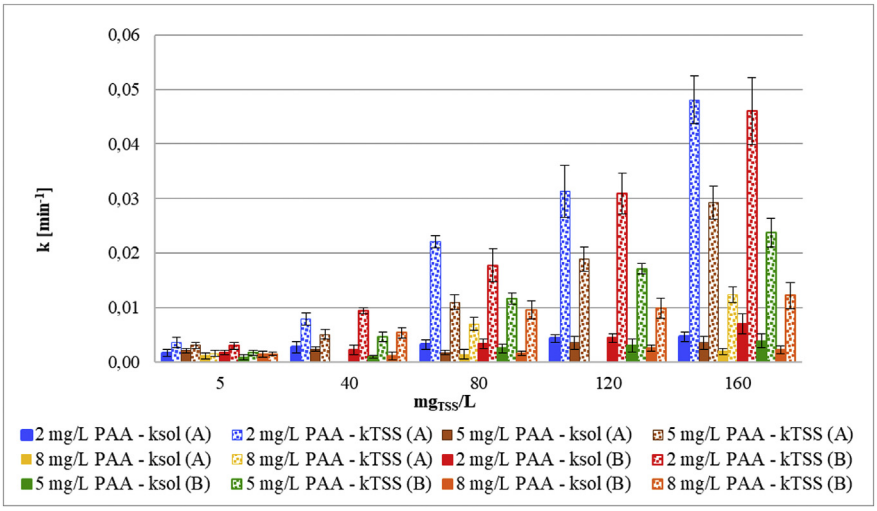

Fig. 1. Decay rate constants of the Haas and Finch kinetic model (mean ± confidence interval at 95% of significance) as a function of TSS and PAA concentration for PAA decay tests on soluble (k_{sol}) and TSS (k_{TSS}) solutions from WWTP-A (A) and WWTP-B (B).

and k_{sol} values for 5 and 40 mg/L at the three initial PAA concentrations were comparable to k_{blank}. The lack of statistically significant differences was proven by an ANOVA test (p-value < 0.05).

At TSS concentrations higher than 40 mg/L the effect of the suspended matter on PAA decay became more relevant, showing an increasing trend with TSS concentrations. Indeed, k_{TSS} values are about five times higher than k_{sol} values at TSS concentrations higher than 40 mg/L, evidencing that TSS content is the main driver of observed PAA decay. Moreover, higher PAA concentrations led to lower values of decay rate constants, thus a slower PAA decay. This trend has also been observed in previous studies (Domínguez Henao et al., 2018; Pedersen et al., 2009) during blank decay tests of PAA at different initial concentrations. It was hypothesized that the higher the PAA concentration the more stable it is in solution.

As for the effect of the source of activated sludge, similar values for decay rate constants were obtained for both WWTPs. Indeed, no significant differences were observed between the experimental data from different WWTPs and the confidence intervals at 95% of significance of the parameters overlap for the experiments at the same TSS and PAA concentrations. Again, the lack of statistically significant differences was assessed by an ANOVA test (p-value < 0.05).

Subsequently, a model was developed to relate the decay rate constant with TSS concentration, composed of two sub-models separately describing the effect of suspended and soluble matter. The choice to describe the effect of suspended and soluble matter as two additive elements was based on the independence that was observed between the two components and on the likely assumption of negligible mutual interaction, as observed by Dignac et al. (2000). In the following, the structure of each sub-model is detailed and the results of the regressions performed on experimental data are reported.

As for the contribution of soluble matter on decay rate constant, it was effectively described based on COD concentration (COD_{sol}). A linear relationship was observed between the decay rate constants normalized by the blank decay rate (k_{sol}/k_{blank}) and COD_{sol}. According to the linear regression, the sub-model formulation is reported in Eq. (3). As observed in a previous work (Domínguez Henao et al., 2018), the COD itself is not an effective predictor for PAA decay since it does not allow to discriminate the effect of the different organic macromolecules (carbohydrates, lipids, protein and nucleic acids) on PAA decay. According to the findings of the aforementioned work, only proteins are the main drivers of PAA consumption.

However, since the effect of the soluble fraction associated to TSS was evaluated adopting different dilution factors from the same stock filtrate solution, it can be assumed that the different COD concentrations are proportional to the concentration of soluble matter affecting PAA decay. Moreover, a linear dependence on initial PAA concentration was highlighted, whose effect was incorporated in the term γ, as evidenced in Eq. (4). Finally, the blank decay rate constant was defined as reported in Eq. (5), being the formulation adopted from one determined by Domínguez Henao et al. (2018).

$$\frac{k_{sol}}{k_{blank}} = 1 + \gamma \cdot COD_{sol} \tag{3}$$

$$\gamma = a_1 + a_2 \cdot PAA_0 \tag{4}$$

$$k_{blank} = 0.00128 - 6.24 \cdot 10^{-5} \cdot PAA_0 \tag{5}$$

where COD_{sol} is expressed in mg_{O2}/L, k is the decay rate of PAA, expressed in min^{-1}, and PAA_0 represents the initial PAA concentration expressed in mg/L.

The effect of suspended matter on the decay rate constant was described separately from the soluble part as an independent coefficient k*, as shown in Eq. (6). In detail, under the assumption of independence between effects, the difference between k_{TSS} (overall decay rate ascribable to suspended and soluble matter) and k_{sol} (decay rate ascribable only to soluble matter) represents the decay rate due to suspended matter. A model to describe k* was obtained by means of a non-linear regression on data obtained from the difference between k_{TSS} and k_{sol} normalized by the k_{blank}. The resulting model indicates that the effect of suspended matter depends on TSS concentration and initial PAA concentration. The effect is null in the absence of TSS in solution, as expected.

$$k^* = \frac{k_{TSS} - k_{SOL}}{k_{blank}} = b_1 \cdot TSS^{\alpha} \cdot {PAA_0}^{\beta} \tag{6}$$

where TSS is the concentration of suspended matter (mg/L).

The overall model accounting for the effect of soluble and suspended matter is obtained by merging Eqs. (3), (4) and (5), as presented in Eq. (7), in which k_{TSS} normalized by the k_{blank} is defined:

$$\frac{k_{TSS}}{k_{blank}} = \frac{k_{sol}}{k_{blank}} + k^* = 1 + (a_1 + a_2 \cdot PAA_0) \cdot COD_{sol} + b_1 \cdot TSS^{\alpha} \cdot {PAA_0}^{\beta} \tag{7}$$

where a_1, a_2, b_1, α and β are the coefficients of the non-linear regression. The results of regressions on the dataset from each WWTP (parameter estimates and main statistics) are reported in Supporting Material for the sub-model for soluble matter (Table S3), for the sub-model for

Table 3
Main statistics and regression estimates for the overall model of the effect of suspended and soluble matter on PAA decay rate constant obtained from the single pooled dataset of both WWTPs.

Parameter	Soluble matter model		Suspended matter model		
	a_1	a_2	b_1	α	β
Estimates	0.062	−0.006	0.085	1.263	−0.543
Min 95% confidence interval	0.044	−0.009	0.044	1.165	−0.609
Max 95% confidence interval	0.079	−0.002	0.125	1.36	−0.476
Standard error (SE)	0.009	0.002	0.021	0.049	0.034
t (df)	7.03	−3.505	4.074	25.59	−16.086
p-level	<e-11	<e-04	<e-05	<e-58	<e-35
R^2 (adj-R^2)	0.964 (0.963)				
n	164				

suspended matter (Table S4), and for the overall model (Table S5). In addition to the effectiveness of both sub-models in describing the related phenomena, satisfactory results were obtained by the overall model (R^2 values equal to 0.972 and 0.965, respectively for WWTP-A and WWTP-B).

Since confidence intervals at 95% of significance for estimated parameters overlap between WWTP-A and WWTP-B, it was hypothesized that there are not significant differences between the two WWTPs, therefore all the experimental data was analyzed as a single pooled dataset. Results of regression are reported in Table 3, while a graphical representation of the overall model is shown in Fig. 2.

The overall model obtained from the single pooled dataset of WWTPs is effective in describing the effect of suspended and soluble matter on PAA decay rate constant, as highlighted by the high R^2 value. The negative values of a_2 and β coefficients indicate that the detrimental effect is more pronounced at low initial PAA concentrations, which is in agreement with the idea of a consumption mechanism determined by the reaction of PAA molecules with other compounds, suspended or dissolved.

It is interesting to observe that, according to the interpolated model, the presence of 40 mg/L of TSS causes decreases within 60 min of 16, 7 and 4% of PAA initial concentrations of 2, 5, 8 mg/L, respectively. The decrease of the same initial PAA concentration turns into 61, 41 and 29% respectively in the presence of 160 mg/L of TSS. This evidences the effect of TSS content on PAA decay, which stresses the importance of an efficient settling process for suspended matter removal in order to optimize the disinfectant dosage. Furthermore, this outcome entails that, when dealing with effluents with high content of suspended matter, the measurement of the TSS concentration is a reliable and easy-to-measure parameter to determine the decay rate and therefore the half-life of a defined PAA initial concentration.

Lastly, an uncertainty analysis was performed by a series of Monte Carlo simulations to propagate the uncertainties associated to the coefficients of the model on the output, in an analogous way as reported in a previous work (Domínguez Henao et al., 2018). In detail, $7 \cdot 10^4$ lives of the system were simulated for each combination of TSS and PAA concentrations assuming a normal probability distribution functions for the coefficients. In addition, the correlation between the coefficients was taken into account by the correlation matrixes obtained from the regression.

Consequently, for each combination of TSS and PAA concentrations, $7 \cdot 10^4$ different decay rate constants (k) and PAA decay profiles have been obtained. The different PAA concentration values computed at each contact time has been analyzed from a frequent point of view and the data was fitted with a probability density function (pdf). A Generalized Extreme Value (GEV) pdf was found to fit the data better than the normal pdf assumed for the coefficients, which might be due to the non-linear nature of the model. According to this hypothesis, a confidence interval at 95% confidence has been estimated.

As an example, frequency histograms of Monte Carlo simulation results for 2 mg/L of PAA and 160 mg/L of TSS at five different contact times (2, 5, 10, 30 and 60 min) and the related interpolations with GEV pdf are shown in Fig. 3.

3.2. *E. coli* inactivation

3.2.1. Dose-response curve

Disinfection tests for building the dose-response curve were performed in saline solution, in which PAA alone interacts with bacteria and no other compound interferes with the disinfection process. Furthermore, the saline solution is isotonic with the bacterial cells, which nullifies the osmotic stress to the cells. The response of *E. coli* when

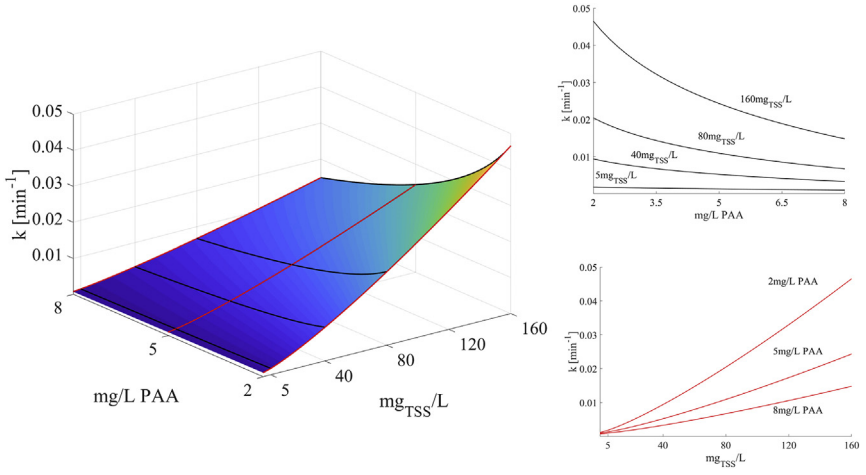

Fig. 2. 3D (left) and 2D (right) plots of the overall model of the effect of suspended and soluble matter on PAA decay rate constant as a function of TSS concentration and initial PAA concentration.

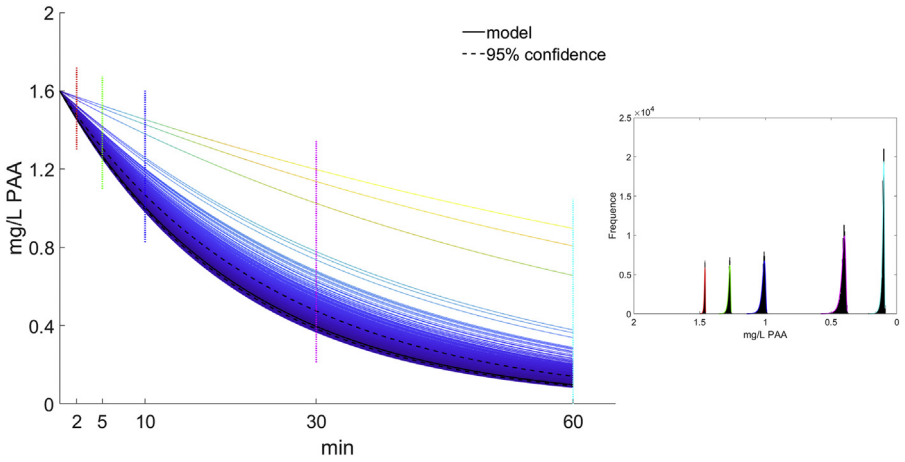

Fig. 3. Results of the exemplary Monte Carlo analysis for $7 \cdot 10^4$ simulations (2 mg/L of PAA and 160 mg/L of TSS). Computed PAA decay profiles over time (left); output distribution (approximated by a GEV pdf) of the model at five different sections (2, 5, 10, 30 and 60 min).

exposed to different PAA doses (5, 10, 15, 20 and 25 mg/L min) determined in saline solution is presented in Fig. 4, where the log-inactivation ($\log N/N_0$) values are presented as a function of PAA dose.

In detail, D_{PAA} was changed by varying the contact time at the same initial PAA concentration (PAA_0), while taking into account the PAA decay in saline solution, which was assumed to be equivalent to the blank decay (k_{blank}) determined by Eq. (5) since it is not expected that physiological salinity has any effect on PAA decay. Experimental results indicated that, after an initial lag of inactivity, *E. coli* followed a rapid inactivation by PAA. Log-inactivation values ranged from −0.6 to −5.3, depending on the applied PAA dose. Comparable levels of *E. coli* inactivation for similar PAA doses were observed in the study of McFadden et al. (2017), in which the same strain of *E. coli* was used, whereas a similar level of *E. coli* inactivation required much larger doses in other studies (Rossi et al., 2007; Santoro et al., 2015). The differences in the bacteria behavior can probably be attributed to the use of a pure lab culture of *E. coli*, characterized by a lower resistance to inactivation than heterogeneous mixtures of bacteria naturally present in real effluents.

Nevertheless, a typical sigmoidal-shaped response of *E. coli* was observed, as shown in Fig. 4, in which the initial lag phase is determined by an initial resistance to inactivation, followed by an exponential inactivation phase where the maximum inactivation rate is achieved, and finally by an asymptotic inactivation phase, during which the inactivation rate decreases (Mezzanotte et al., 2007). The initial shoulder trend is usually attributed to the diffusion resistance of PAA through the cell membrane, which delays the inactivation effect (Rossi et al., 2007). Previous studies of PAA inactivation reported similar trends of initial lag phase in the presence of low doses of PAA (McFadden et al., 2017; Rossi et al., 2007; Santoro et al., 2005). On the other hand, the final tailing-off trend is commonly explained by the presence of suspended solids or a genetic heterogeneity of microorganisms, resulting in different capacities of resistance to disinfectant (Profaizer, 1998; Rossi et al., 2007). However, in this specific case, previous reasons could not explain the tailing-off trend because only NaCl is present in saline solution and only one type of DNA characterizes the *E. coli* culture. Therefore, it can be hypothesized that the trend is caused by bacterial aggregation. Indeed, bacteria tend naturally to aggregate in natural environments as protection mechanism against extreme conditions (Bohrerova and Linden, 2006; Mir et al., 1997). Consequently, bacteria located in the external part of the aggregate can be inactivated by the disinfectant, whilst bacteria in the core of the aggregate might survive to PAA disinfection.

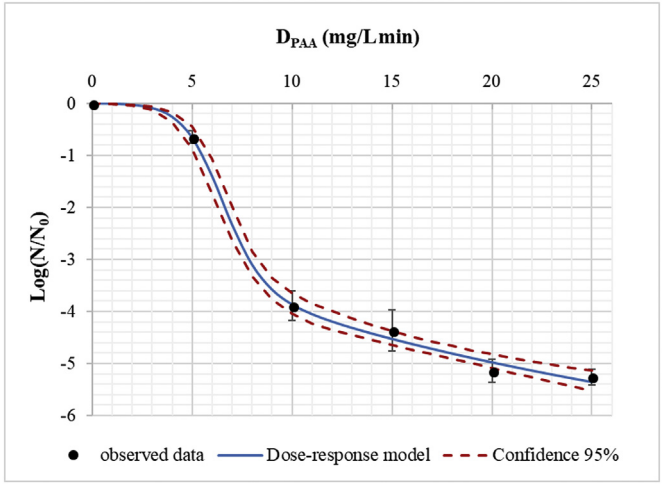

Fig. 4. *E. coli* log-inactivation in saline solution at different PAA doses: experimental (mean ± standard deviation) and modeled data. Confidence intervals at 95% of significance are reported.

Some of the most commonly used inactivation models belong to a family of special cases of the generalized inactivation rate (GIR) model, according to Eq. (8) (Gyürék and Finch, 1998; Li, 2004; Santoro et al., 2007).

$$\frac{dN}{dt} = -k' C^n m N^x t^{m-1} \tag{8}$$

where k′ is the bacterial inactivation rate constant, *n*, *m* and *x* are model parameters, *C* is the disinfectant concentration and *t* is the contact time. The GIR parameters lead to the different inactivation models, namely Chick-Watson, Hom, Power Law (Rational) and Hom Power Law (HPL), which can be combined with the disinfectant decay kinetics, in order to consider the loss of disinfectant in time. The inactivation equations with the disinfectant demand and their integrated solutions have been described in previous works (Gyürék and Finch, 1998; Haas et al., 1995; Haas and Joffe, 1994; Jacangelo et al., 2002), providing a suitable option to consider the disinfectant loss during bacterial inactivation. However, analytical solutions may be not available for all disinfectant decay kinetics (Haas and Joffe, 1994; Jacangelo et al., 2002; Santoro et al., 2007) and further assumptions are required to obtain a closed form of the inactivation models, such as (1) negligible instantaneous disinfectant demand and (2) negligible microbial inactivation during instantaneous disinfectant demand (Santoro et al., 2007). Under these assumptions, inactivation models accounting for zero-order disinfectant decay have been adopted in the past (Anotai, 1996; Santoro et al., 2007).

Moreover, considering both the disinfectant decay and inactivation models, such as the Rational and the HPL, result in expressions that are complex with as many as four parameters that can lead to

overparametrization, resulting in highly correlated parameter estimates (Bates and Watts, 1988; Gyürék and Finch, 1998).

Most of these models have been developed and studied for chlorine or ozone; therefore, some assumptions are not suitable for PAA disinfection. For instance, PAA decay generally follows the first-order kinetic rate law as described previously and as found in previous works (Antonelli et al., 2006; Falsanisi et al., 2006; Luukkonen and Pehkonen, 2016; Rossi et al., 2007) and for effluents with high organic or TSS content the instantaneous disinfectant demand cannot be neglected.

The S-model for PAA disinfection kinetics proposed by Profaizer (1998), on the other hand, takes into account the decay, however it considers the applied PAA concentration and contact time as independent variables.

Considering that an essential feature of kinetic modeling is simplification and idealization of complex phenomena, a log-inactivation model to describe experimental data on *E. coli* inactivation as a function of the PAA dose has been defined in the present work, whose formulation is reported in Eq. (9).

$$\log\left(\frac{N}{N_0}\right) = -k' \cdot {D_{PAA}}^{n} \cdot \left(\frac{1}{1+e^{h-D_{PAA}}}\right) \tag{9}$$

where D_{PAA} (mg/L min) is the PAA dose at which bacteria are exposed determined by Eq. (2), and k', n and h are the empirical model parameters. In detail, the model has been built assuming that the log-inactivation could be described in two parts. The first one can be regarded as a special case of the GIR, where $m, x = 1$ and in which (i) the disinfectant concentration and contact time have the same weight at defining the log-inactivation and (ii) the product of the C and t can be approximated to D_{PAA}, as the effective exposure dose. However, this expression alone is not yet satisfactory to fit the inactivation data. Therefore, the second part that corresponds to a sigmoid function, contributes to the definition of the typical disinfection S-shaped dose-response curve, in a similar fashion as the inactivation model proposed by Profaizer (1998), in which the parameter h determines the initial lag phase of the inactivation curve at low doses (shoulder trend). It is noteworthy that when $D_{PAA} < h$ in Eq. (9), the denominator takes values higher than 1 resulting in the shoulder trend. This effect becomes negligible at high D_{PAA} values ($D_{PAA} > h$), as shown in Fig. 5.

The parameters of the proposed model for log-inactivation of *E. coli* due to PAA disinfection were estimated by a non-linear regression of the experimental data. Table 4 summarizes the main statistics and the regression estimates, while the modeled data are reported in Fig. 4.

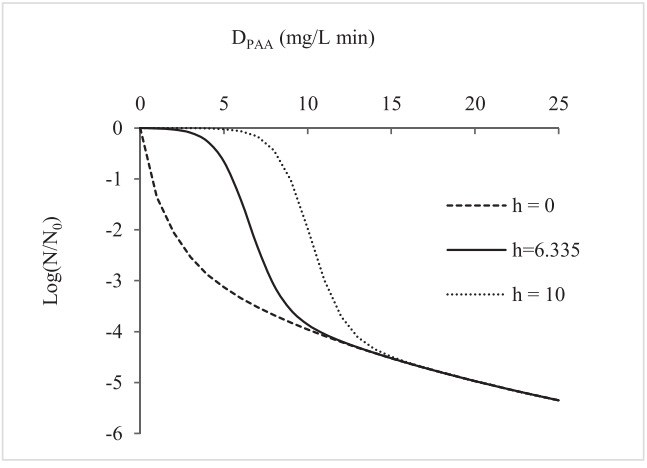

Fig. 5. Graphical study of the behavior of the proposed model for log-inactivation of *E. coli* due to PAA disinfection as a function of parameter h.

Table 4
Main statistics and regression estimates of the dose-response model for *E. coli*.

Parameter	k′	n	h
Estimates	1.851	0.328	6.335
Min 95% confidence interval	1.404	0.246	5.885
Max 95% confidence interval	2.297	0.412	6.785
Standard error (SE)	0.215	0.040	0.218
t (df)	8.576	8.215	29.101
p level	<0.05	<0.05	<0.05
R^2 (Adj-R^2)	0.990 (0.989)		
n	26		

3.2.2. Independence of *E. coli* inactivation from operating conditions at a fixed D_{PAA}

Similar inactivation levels were obtained for all the combinations tested for 20 mg/L min with log-inactivation values of -4.92 ± 0.26 (mean $\pm$ standard deviation), as shown in Fig. 6. An ANOVA for 20 mg/L min did not show significant differences namong log-inactivation values observed for different combinations of initial PAA concentration and contact time for a defined dose (p-value of 0.334). Conversely, at 5 mg/L min an ANOVA showed significant differences among the inactivation values (p-values 0.002). Indeed, a graphical inspection of Fig. 6 evidences a much higher inactivation for combination #5 ($[PAA]_0 =$ 0.09 mg/L, $t = 60$ min). The statistical analysis of the dataset for 5 mg/L min excluding combination #5 evidenced that there are no differences among log-inactivation values (p-value 0.067). Consequently, only combination #5 for the lowest PAA dose led to different levels of inactivation than its peers, displaying higher log-inactivation (-1.53 ± 0.46) with respect to the average value obtained for other combinations (-0.59 ± 0.12). Therefore, the level of *E. coli* inactivation obtained for a defined PAA dose was independent from operating conditions PAA_0 and t, up to 45 min for 5 mg/L min and 60 min and 20 mg/L min.

3.2.3. Effect of TSS on PAA disinfection

The effect of TSS on PAA disinfection was assessed on free-swimming *E. coli* and it was assumed that no PAB was present since the cell suspension of the *E. coli* culture was spiked in the test solution at the beginning of the trial. Indeed, PAB would require prior incubation time to develop within the pores of the particle (LeChevallier et al., 1984), in order to produce extracellular polymers to attach themselves on the surface of the particle. Moreover, PAB growth is limited by the average size of the particles present in the solution and they are expected to be protected by TSS larger than 10 μm: this is the conventional size threshold dividing free-swimming bacteria from PAB (Emerick et al., 2000; Falsanisi et al., 2008).

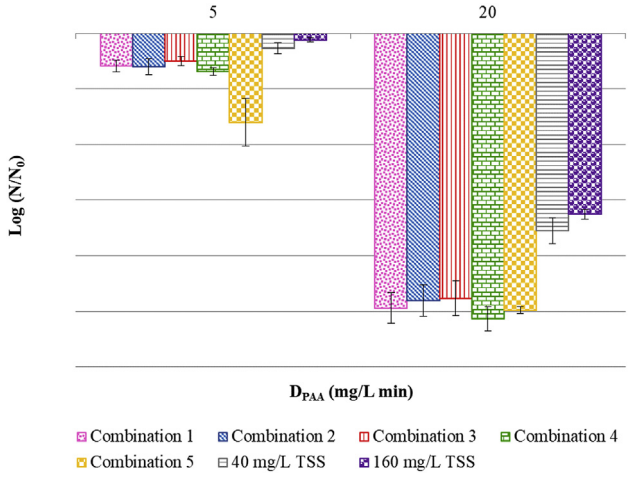

Fig. 6. *E. coli* log-inactivation (mean $\pm$ standard deviation) in saline solution, 40 and 160 mg/L of TSS for different combinations of PAA_0 and contact time at defined PAA doses.

Disinfection tests in saline solution quantified the log-inactivation at defined PAA doses without any other factor affecting the process, as described previously. Therefore, in case that PAA dose is the main factor determining log-inactivation of free-swimming bacteria, similar values are expected in both saline solution and in the presence of TSS.

As shown in Fig. 6, lower log-inactivation values were observed in the presence of both concentrations of TSS tested (40 and 160 mg/L) compared to the values in saline solution at same PAA doses. The protection afforded by TSS to *E. coli* showed to be dependent on PAA dose. At 5 mg/L min the presence of 40 and 160 mg/L of TSS afforded a protection of approximately 0.33 and 0.48 logs respectively, whereas at 20 mg/L min the same concentrations of TSS increased the protection to 1.37 and 1.67 logs, respectively. A *t*-test between log-inactivation values at two TSS concentrations confirmed significant statistical differences at each PAA dose (*p*-values equal to 0.027 and 0.033 at 5 and 20 mg/L min, respectively).

Consequently, the presence of TSS in solution affects the disinfection efficiency of free-swimming bacteria, beyond its effect on PAA decay that was accounted for in the calculation of PAA dose according to Eq. (2). This can be attributed to a protection mechanism afforded to bacteria.

The mechanism of protection afforded by TSS to bacteria (free-swimming and PAB) is not thoroughly understood and many efforts have been addressed to elucidate it. It has been hypothesized that TSS effect on disinfection was due to PAA decay, leading bacteria to be exposed to lower doses of disinfectant (Chhetri et al., 2016, 2014). Experiments performed at same levels of PAA dose allow excluding this mechanism and proved the occurrence of interaction phenomena between bacteria and solids. According to a previous work (LeChevallier et al., 1984), 20% of the dispersed *E. coli* can attach to a porous material in 20 min and find protection from disinfectant action. In this case, since the size of TSS is comparable to bacteria size, this hypothesis is ruled out. Therefore, it can be hypothesized that TSS act as a condensation nucleus and that they are able to favor aggregation of bacteria, as already observed for disinfection with PAA and other disinfectants (Bohrerova and Linden, 2006; Mir et al., 1997; Turolla et al., 2017).

4. Conclusions

The effect of TSS on PAA decay was studied. Increasing TSS concentrations lead to higher PAA decay rates, trend that becomes more pronounced at TSS concentrations above 40 mg/L and a non-linear regression was performed to interpolate a model to describe this behavior. As for the contribution of the associated soluble matter to PAA decay, it displayed a linear relationship with soluble COD and its effect was found to be additive to the one of the TSS, yet much less relevant particularly at high TSS concentrations. This outcome suggests that when implementing PAA for the disinfection of effluents with high solid load, such as primary effluents and sewer overflows, TSS concentration allows determining the PAA consumption.

Regarding the adoption of D_{PAA} as the main parameter determining disinfection efficiency, it proved to be invariant from the combination of initial concentration of PAA and contact time up to 45 min for the lowest dose tested (5 mg/L min) and up to 60 min for higher doses (20 mg/L min).

As for the role of the TSS during *E. coli* inactivation by PAA, a detrimental effect was observed given that the presence of TSS lead to lower bacterial abatements respect to ones observed in saline solution. This effect was dependent on both TSS concentration and PAA dose. In detail, a more pronounced protective effect by TSS was observed at higher PAA doses, which suggests that the protection afforded might be proportional to the PAA dose applied.

Further studies are required to elucidate the protection mechanism afforded by TSS to bacteria against the disinfection and their role as potential condensation nucleus promoting bacterial aggregation.

Acknowledgements

The research activity was supported by the company PeroxyChem (Philadelphia, USA) and by Fondazione Cariplo (DrinkAble project, grant # 2014-1285). Prof. Andrea Franzetti (Università degli Studi di Milano - Bicocca), Dr. Andrea Di Cesare and Dr. Gianluca Corno (Microbial Ecology Group, Institute of Ecosystem Study, National Research Council, Verbania, Italy) are gratefully acknowledge for their guidance in the preparation of the *E. coli* culture. The valuable support of Riccardo Delli Compagni (Politecnico di Milano) for the uncertainty analysis is acknowledged.

Appendix A. Supplementary data

Supplementary data to this article can be found online at https://doi.org/10.1016/j.scitotenv.2018.06.219.

References

Anotai, J., 1996. Effect of Calcium Ion on Chemistry and Disinfection Efficiency of Free Chlorine. PhD. Dissertation. Drexel University.

Antonelli, M., Rossi, S., Mezzanotte, V., Nurizzo, C., 2006. Secondary effluent disinfection: PAA long term efficiency. Environ. Sci. Technol. 40:4771–4775. https://doi.org/10.1021/es060273f.

APAT-IRSA/CNR, 2003. Metodi analitici per il controllo della qualità delle acque. Rome, Italy.

APHA/AWA/WEF, 2012. Standard Methods for the Examination of Water and Wastewater. 22nd Ed. American Public Health Association; American Water Works Association; Water Environment Federation, Washington, DC (doi:ISBN 9780875532356).

Bates, D.M., Watts, D.G., 1988. Nonlinear Regression Analysis and Its Applications. https://doi.org/10.1002/9780470316757.ch2.

Bohrerova, Z., Linden, K.G., 2006. Ultraviolet and chlorine disinfection of Mycobacterium in wastewater: effect of aggregation. Water Environ. Res. 78:565–571. https://doi.org/10.2175/106143006X99795.

Chhetri, R.K., Thornberg, D., Berner, J., Gramstad, R., Öjstedt, U., Sharma, A.K., Andersen, H. R., 2014. Chemical disinfection of combined sewer overflow waters using performic acid or peracetic acids. Sci. Total Environ. 490:1065–1072. https://doi.org/10.1016/j.scitotenv.2014.05.079.

Chhetri, R.K., Bonnerup, A., Andersen, H.R., 2016. Combined sewer overflow pretreatment with chemical coagulation and a particle settler for improved peracetic acid disinfection. J. Ind. Eng. Chem. 37:372–379. https://doi.org/10.1016/j.jiec.2016.03.049.

Dell'Erba, A., Falsanisi, D., Liberti, L., Notarnicola, M., Santoro, D., 2007. Disinfection by-products formation during wastewater disinfection with peracetic acid. Desalination 215:177–186. https://doi.org/10.1016/j.desal.2006.08.021.

Dietrich, J.P., Başağaoğlu, H., Loge, F.J., Ginn, T.R., 2003. Preliminary assessment of transport processes influencing the penetration of chlorine into wastewater particles and the subsequent inactivation of particle-associated organisms. Water Res. 37:139–149. https://doi.org/10.1016/S0043-1354(02)00239-7.

Dietrich, J.P., Loge, F.J., Ginn, T.R., Başağaoğlu, H., 2007. Inactivation of particle-associated microorganisms in wastewater disinfection: modeling of ozone and chlorine reactive diffusive transport in polydispersed suspensions. Water Res. 41:2189–2201. https://doi.org/10.1016/j.watres.2007.01.038.

Dignac, M.F., Ginestet, P., Rybacki, D., Bruchet, A., Urbain, V., Scribe, P., 2000. Fate of wastewater organic pollution during activated sludge treatment: nature of residual organic matter. Water Res. 34:4185–4194. https://doi.org/10.1016/S0043-1354(00)00195-0.

Domínguez Henao, L., Delli Compagni, R., Turolla, A., Antonelli, M., 2018. Influence of inorganic and organic compounds on the decay of peracetic acid in wastewater disinfection. Chem. Eng. J. 337:133–142. https://doi.org/10.1016/j.cej.2017.12.074.

Domínguez-Henao, L., Turolla, A., Monticelli, D., Antonelli, M., 2018. Assessment of a colorimetric method for the measurement of low concentrations of peracetic acid and hydrogen peroxide in water. Talanta 183:209–215. https://doi.org/10.1016/j.talanta.2018.02.078.

Emerick, R.W., Loge, F.J., Ginn, T., Darby, J.L., 2000. Modeling the inactivation of particle-associated coliform bacteria. Water Environ. Res. 432–438 (7):72. https://doi.org/10.2175/106143000X137969.

Falsanisi, D., Gehr, R., Santoro, D., Dell'Erba, A., Notarnicola, M., Liberti, L., 2006. Kinetics of PAA demand and its implications on disinfection of wastewaters. Water Qual. Res. J. Canada 41:398–409. https://doi.org/10.2166/wqrj.2006.043.

Falsanisi, D., Gehr, R., Liberti, L., Notarnicola, M., 2008. Effect of suspended particles on disinfection of a physicochemical municipal wastewater with peracetic acid. Water Qual. Res. J. Canada 43:47–54. https://doi.org/10.2166/wqrj.2008.006.

Gehr, R., Cochrane, D., 2002. Peracetic acid (PAA) as a disinfectant for municipal wastewaters: encouraging performance results from physicochemical as well as biological effluents. Proc. Water Environ. Fed. 2002:182–198. https://doi.org/10.2175/193864702785033527.

Gyürék, L.L., Finch, G.R., 1998. Modelling water treatment chemical disnfection kinetics. J. Environ. Eng. 124:783–793. https://doi.org/10.1061/(ASCE)0733-9372(1998)124:9(783).

Haas, C.N., Finch, G.R., 2001. Methodologies for the Determination of Disinfection Effectiveness. AWWA Research Foundation and American Water Works Association.

Haas, C.N., Joffe, J., 1994. Disinfection under dynamic conditions: modification of Hom's model for decay. Environ. Sci. Technol. 28:1367–1369. https://doi.org/10.1021/es00056a028.

Haas, C.N., Heath, M.S., Jacangelo, J., Joffe, J., Anmangandla, U., Hornberger, J.C., Glicker, J., 1995. Development and Validation of Rational Design Methods of Disinfection. The Foundation and American Water Works Association, Denver, CO.

Jacangelo, J.G., Patania, N., Trussell, R., Gerba, C., Haas, C.N., 2002. Inactivation of Waterborne Emerging Pathogens by Selected Disinfectants. AWWA Research Foundation and American Water Works Association, Denver, CO.

Kitis, M., 2004. Disinfection of wastewater with peracetic acid: a review. Environ. Int. 30: 47–55. https://doi.org/10.1016/S0160-4120(03)00147-8.

Koivunen, J., Heinonen-Tanski, H., 2005. Peracetic acid (PAA) disinfection of primary, secondary and tertiary treated municipal wastewaters. Water Res. 39:4445–4453. https://doi.org/10.1016/j.watres.2005.08.016.

Lazarova, V., Janex, M., Fiksdal, L., Oberg, C., Barcina, I., Pommepuy, M., 1998. Advanced wastewater disinfection technologies: short and long term efficiency. Water Sci. Technol. 38:109–117. https://doi.org/10.1016/S0273-1223(98)00810-5.

LeChevallier, M.W., Hassenauer, T.S., Camper, A.K., McFeters, G.A., 1984. Disinfection of bacteria attached to granular activated carbon. Appl. Environ. Microbiol. 48, 918–923.

Lefevre, F., Audic, J.M., Ferrand, F., 1992. Peracetic acid disinfection of secondary effluents discharged off coastal seawater. Water Sci. Technol. 25, 155–164.

Li, L., 2004. Effects of Initial Microbial Density on Disinfection Efficiency in a Continuous Flow System and Validation of Disinfection Batch Kinetics in a Continuous Flow System. PhD. Dissertation. Drexel University.

Liberti, L., Notarnicola, M., 1999. Advanced treatment and disinfection for municipal wastewater reuse in agriculture. Water Sci. Technol. 40:235–245. https://doi.org/10.1016/S0273-1223(99)00505-3.

Liu, D., Steinberg, C., Straus, D.L., Pedersen, L., Meinelt, T., 2014. Salinity, dissolved organic carbon and water hardness affect peracetic acid (PAA) degradation in aqueous solutions. Aquac. Eng. 60:35–40. https://doi.org/10.1016/j.aquaeng.2014.03.006.

Luukkonen, T., Pehkonen, S.O., 2016. Peracids in water treatment: a critical review. Crit. Rev. Environ. Sci. Technol. 0:1–39. https://doi.org/10.1080/10643389.2016.1272343.

Luukkonen, T., Teeriniemi, J., Prokkola, H., Rämö, J., Lassi, U., 2014. Chemical aspects of peracetic acid based wastewater disinfection. Water SA 40:73–80. https://doi.org/10.4314/wsa.v40i1.9.

McFadden, M., Loconsole, J., Schockling, A.J., Nerenberg, R., Pavissich, J.P., 2017. Comparing peracetic acid and hypochlorite for disinfection of combined sewer overflows: effects of suspended-solids and pH. Sci. Total Environ. 599–600:533–539. https://doi.org/10.1016/j.scitotenv.2017.04.179.

Mezzanotte, V., Antonelli, M., Citterio, S., Nurizzo, C., 2007. Wastewater disinfection alternatives : chlorine, ozone, Peracetic acid, and UV light. Water Environ. Res. 79: 2373–2379. https://doi.org/10.2175/106143007X183763.

Mir, J., Morató, J., Ribas, F., 1997. Resistance to chlorine of freshwater bacterial strains. J. Appl. Microbiol. 82:7–18. https://doi.org/10.1111/j.1365-2672.1997.tb03292.x.

Pedersen, L.F., Pedersen, P.B., Nielsen, J.L., Nielsen, P.H., 2009. Peracetic acid degradation and effects on nitrification in recirculating aquaculture systems. Aquaculture 296: 246–254. https://doi.org/10.1016/j.aquaculture.2009.08.021.

Pedersen, L.F., Meinelt, T., Straus, D.L., 2013. Peracetic acid degradation in freshwater aquaculture systems and possible practical implications. Aquac. Eng. 53:65–71. https://doi.org/10.1016/j.aquaeng.2012.11.011.

Profaizer, M., 1998. Peracetic Acid as an Alternative Technology for Drinking Water Disinfection: A New Modelling Approach (in Italian). PhD. Dissertation. Politecnico di Milano.

Qualls, R.G., Flynn, M.P., Johnson, J.D., Flynn, P., Donald, J., Quails, R.G., 1983. The role of suspended particles in ultraviolet disinfection. Water Pollut. Control Fed. 55: 1280–1285. https://doi.org/10.2307/25042084.

Qualls, R.G., Ossoff, S.F., Chang, J.C.H., Dorfman, M.H., Dumais, C.M., Lobe, D.C., Johnson, J. D., 1985. Factors controlling censitivity in ultraviolet disinfection of secondary effluents. J. Water Pollut. Control Fed. 57:1006–1011. https://doi.org/10.2307/25042770.

Rossi, S., Antonelli, M., Mezzanotte, V., Nurizzo, C., 2007. Peracetic acid disinfection: a feasible alternative to wastewater chlorination. Water Environ. Res. 79:341–350. https://doi.org/10.2175/106143006X101953.

Sánchez-Ruiz, C., Martínez-Royano, S., Tejero-Monzón, I., 1995. An evaluation of the efficiency and impact of raw wastewater disinfection with peracetic acid prior to ocean discharge. Water Sci. Technol. 32:159 LP–166. https://doi.org/10.1016/0273-1223(96)00060-1.

Santoro, D., Bartrand, T.A., Greene, D.J., Farouk, B., Haas, C.N., Notarnicola, M., Liberti, L., 2005. Use of CFD for wastewater disinfection process analysis: *E. coli* inactivation with peroxyacetic acid (PAA). Int. J. Chem. React. Eng. 3, 14. https://doi.org/10.2202/1542-6580.1283.

Santoro, D., Gehr, R., Bartrand, T.A., Liberti, L., Notarnicola, M., Dell'Erba, A., Falsanisi, D., Haas, C.N., 2007. Wastewater disinfection by peracetic acid: assessment of models for tracking residual measurements and inactivation. Water Environ. Res. 79: 775–787. https://doi.org/10.2175/106143007X156817.

Santoro, D., Crapulli, F., Raisee, M., Raspa, G., Haas, C.N., 2015. Nondeterministic computational fluid dynamics modeling of *Escherichia coli* inactivation by Peracetic acid in municipal wastewater contact tanks. Environ. Sci. Technol. 49:7265–7275. https://doi.org/10.1021/es5059742.

Stampi, S., De Luca, G., Zanetti, F., 2001. Evaluation of the efficiency of peracetic acid in the disinfection of sewage effluents. J. Appl. Microbiol. 91, 833–838.

Sully, B.D., Williams, P.L., 1962. The analysis of solutions of per-acids and hydrogen peroxide. Analyst 87:653. https://doi.org/10.1039/an9628700653.

Turolla, A., Sabatino, R., Fontaneto, D., Eckert, E.M., Colinas, N., Corno, G., Citterio, B., Biavasco, F., Antonelli, M., Mauro, A., Mangiaterra, G., Di Cesare, A., 2017. Defence strategies and antibiotic resistance gene abundance in enterococci under stress by exposure to low doses of peracetic acid. Chemosphere 185:480–488. https://doi.org/10.1016/j.chemosphere.2017.07.032.

US EPA, 1999. Combined Sewer Overflow Technology Fact Sheet. United States Environ. Prot. Agency, Washingt. DC, USA (doi:EPA 832-F-99-041).

Winward, G.P., Avery, L.M., Stephenson, T., Jefferson, B., 2008. Chlorine disinfection of grey water for reuse: effect of organics and particles. Water Res. 42:483–491. https://doi.org/10.1016/j.watres.2007.07.042.

Yuan, Z., Ni, Y., Van Heiningen, A.R., 1997. Kinetics of the peracetic acid decomposition: part II: pH effect and alkaline hydrolysis. Can. J. Chem. Eng. 75:42–47. https://doi.org/10.1002/cjce.5450750109.